

Nuclear and Coulomb Interaction in ^8B Breakup at Sub-Coulomb Energies

V. Guimarães, J. J. Kolata, D. Peterson, P. Santi, R. H. White-Stevens, and S. M. Vincent

Physics Department, University of Notre Dame, Notre Dame, Indiana 46556-5670

F. D. Becchetti, M. Y. Lee, T. W. O'Donnell, D. A. Roberts, and J. A. Zimmerman

Physics Department, University of Michigan, Ann Arbor, Michigan 48109-1120

(Received 24 September 1999)

The angular distribution for the breakup of $^8\text{B} \rightarrow ^7\text{Be} + p$ on a ^{58}Ni target has been measured at an incident energy of 25.75 MeV. The data are inconsistent with first-order theories but are remarkably well described by calculations including higher-order effects. The comparison with theory illustrates the importance of the inclusion of the exotic proton halo structure of ^8B in accounting for the data.

PACS numbers: 25.60.Gc, 21.10.Gv, 27.20.+n

Coulomb dissociation reactions have been used in recent years as a means to obtain information on capture reactions of astrophysical interest. An example is the experiment of Motobayashi *et al.* [1] who studied the breakup of $^8\text{B} \rightarrow ^7\text{Be} + p$ on a Pb target and related their result to radiative proton capture at solar energies. This reaction corresponds to the projectile breaking up into a core and a valence nucleon due to interactions with virtual photons in the strong Coulomb field of a high- Z nucleus. Although this mechanism is, in principle, a time-reversed capture reaction, $E2$ photons contribute to Coulomb dissociation while radiative capture at solar energies proceeds almost exclusively by $E1$ transitions. Thus, in extracting information on astrophysical proton capture reactions from the measured dissociation cross section, it is crucial to determine the relative contribution of photons having different multipolarity.

The relative importance of $E1$ and $E2$ contributions to the Coulomb dissociation of ^8B has been investigated both experimentally [2–5] and theoretically [6–8]. The earliest experiments [2,3] suggested that the $E2$ strength was much smaller than all published theoretical estimates. Davids *et al.* [4] measured the asymmetry in the longitudinal momentum distribution of ^7Be fragments from the dissociation of ^8B on Pb at 44 and 81 MeV per nucleon. The 44 MeV/nucleon data gave a clear signal corresponding to an $E2$ strength that was 70% of that predicted by the model of Esbensen and Bertsch [8]. This model prediction itself is a factor of 2 smaller than that of Kim *et al.* [9]. Nevertheless the extracted $E2$ strength, though considerably quenched, is still larger than implied in Refs. [2] and [3]. Most recently, Iwasa *et al.* [5] report a limit on the $E2$ strength that is at least an order of magnitude smaller than that of Davids *et al.*

It was noted in Ref. [4] that the description of the data by the model of Esbensen and Bertsch is not precise, and that the best-fit values for the $E1$ and $E2$ strengths differ by (20–30)% from the model predictions. The $E2/E1$ interference term is, of course, model dependent. The earlier experiment of von Schwarzenberg *et al.* [2]

attempted to avoid model dependence by measuring the breakup at sub-Coulomb energies for a low- Z target (^{58}Ni) for which multiple Coulomb excitation was expected to be minimal. At these energies, the $E2$ component is enhanced relative to $E1$. The very small cross section reported in that paper, which was less than that predicted by any reasonable structure model for ^8B [10], has generated considerable interest. Nunes and Thompson [10], and Dasso, Lenzi, and Vitturi [11] independently suggested that the explanation for this result might be strong destructive nuclear-Coulomb interference effects, despite the fact that at the angle where the measurement was made the classical distance of closest approach is nearly 20 fm, i.e., far outside the range of the nuclear force for a “normal” nuclear system. A strong nuclear-dominated peak in the differential cross section at a center-of-mass angle of 70° – 90° (well inside the expected 100° – 110° for the onset of nuclear breakup of a normal nucleus) was predicted in Refs. [10] and [11], although it was pointed out that the corresponding calculations are only first order in the nuclear and Coulomb fields and might be modified by multistep excitations. Furthermore, it was suggested in Ref. [10] that even pure Coulomb excitation would be considerably modified from that expected in the normal “point-Coulomb” approximation which ignores the extended size of the valence proton wave function in ^8B (see Ref. [10] for a more complete discussion of this approximation). This leads to a further reduction in the calculated breakup cross section. Both effects are directly attributable to the exotic “halo” structure of ^8B , so it is important to verify, if possible, the implications of these calculations.

The experiment was carried out at the Nuclear Structure Laboratory of the University of Notre Dame. To produce the low-energy secondary radioactive ^8B beam, we used the *TwinSol* radioactive ion beam facility [12] and the $^6\text{Li}(^3\text{He}, n)^8\text{B}$ direct transfer reaction. A gas target containing 1 atm of ^3He was bombarded by a high-intensity (up to 300 particle nA), nanosecond-bunched primary ^6Li beam at an energy of 36 MeV. The entrance

and exit windows of the gas cell consisted of $2.0 \mu\text{m}$ Havar foils. The secondary beam was selected and transported through the solenoids and then focused onto a $924 \mu\text{g}/\text{cm}^2$ thick, isotopically enriched ^{58}Ni secondary target. The laboratory energy of the ^8B beam at the center of this target was 25.75 MeV , with an overall resolution of 0.75 MeV full width at half maximum (FWHM) and an intensity of 2.5×10^4 particles per second. The energy spread was due to a combination of the kinematic shift in the production reaction and energy-loss straggling in the gas-cell windows and the target. The beam had a maximum angular divergence of $\pm 4^\circ$ and a spot size of 4 mm FWHM. Pulse-pileup tagging with a resolving time of 50 ns was used to eliminate pileup events. The ^8B breakup events, and also elastically scattered particles, were detected with two telescopes consisting of 25 and $30 \mu\text{m}$ Si ΔE detectors, backed by thick Si E detectors. These were placed on either side of the beam at $\Theta_{\text{LAB}} = 20^\circ, 30^\circ, 40^\circ, 45^\circ, 50^\circ,$ and 60° . Each telescope had a circular collimator that subtended a solid angle of 41 msr , corresponding to an overall effective angular resolution of 10.9° (FWHM), computed by folding in the acceptance of the collimator with the spot size and angular divergence of the beam.

Unambiguous separation of the ^7Be fragments resulting from ^8B breakup from ^7Be contamination in the direct beam elastically scattered by the ^{58}Ni target was crucial to the success of this experiment. Although contaminants were present in the beam, they could be identified using time-of-flight (TOF) techniques. The TOF of the particles was obtained from the time difference between the occurrence of an E signal in a telescope and the rf timing pulse from the beam buncher. The time resolution of better than 3 ns (FWHM) was adequate to separate ^7Be from ^8B , as illustrated in Fig. 1. At sub-Coulomb energies, it is not easy to carry out a coincidence measurement between the ^7Be fragment and the proton, as was done at higher energies [1,3], due to the much reduced kinematic focusing and lower energy of the protons. Thus, we determined only the integrated ^7Be yield from the dissociation reaction $^8\text{B} \rightarrow ^7\text{Be} + p$. Although the contaminants in the secondary ^8B beam are well separated in the ΔE vs E_{TOTAL} spectrum, as illustrated in Fig. 1(a), it would not have been possible to separate the ^7Be products coming from breakup events from the scattered contaminant ^7Be beam using only this information. However, by also considering the TOF information, particles of different origins could be completely separated, as shown in Fig. 1(b), since the ^7Be from ^8B breakup has the same TOF as the ^8B beam.

The experimental angular distribution deduced for the dissociation of ^8B into $^7\text{Be} + p$ on a ^{58}Ni target is presented in Figs. 2 and 3, as a function of the center-of-mass angle of the detected ^7Be (we used the ^8B elastic-scattering Jacobian to transform the laboratory angles to the center-of-mass frame). The differential cross sections were obtained by integrating ^7Be breakup events over the solid

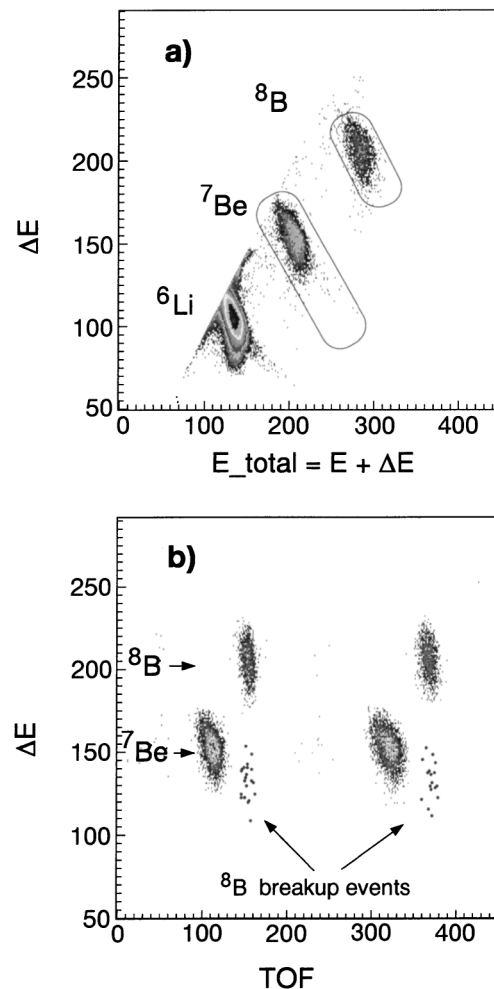


FIG. 1. (a) The ΔE vs E_{TOTAL} spectrum taken at $\Theta_{\text{LAB}} = 45^\circ$. The ^7Be and ^8B gates are shown. (b) TOF- ΔE spectrum illustrating the separation between the ^7Be breakup events and elastically scattered ^7Be in the direct beam. This spectrum corresponds to events in the gates shown in (a). The breakup events are emphasized with larger dots. The energy calibration and time calibration are $20 \text{ keV}/\text{channel}$ and $0.50 \text{ ns}/\text{channel}$, respectively.

angle subtended by the two telescopes. The number of ^8B ions per integrated charge of the primary beam was determined in a separate run. The normalization was obtained using the information on solid angle, target thickness, and integrated charge for each run, and verified by a measurement of ^8B elastic scattering, which is expected to be purely Rutherford at forward angles. The systematic error in the absolute normalization is about 10% , due to the uncertainty in the intensity of the secondary beam. The ^8B beam had a 1° angular offset from the center axis set for the telescopes. This shift, evaluated by analyzing the observed asymmetry in the elastic scattering of ^8B , had a strong effect on the differential cross section at forward angles. Thus, at the most forward angle setting of the telescopes, we display the differential cross sections obtained at $\Theta_{\text{LAB}} = 19^\circ$ and 21° , separately. At backward angles, where the cross section does not change as rapidly as a function of angle, we

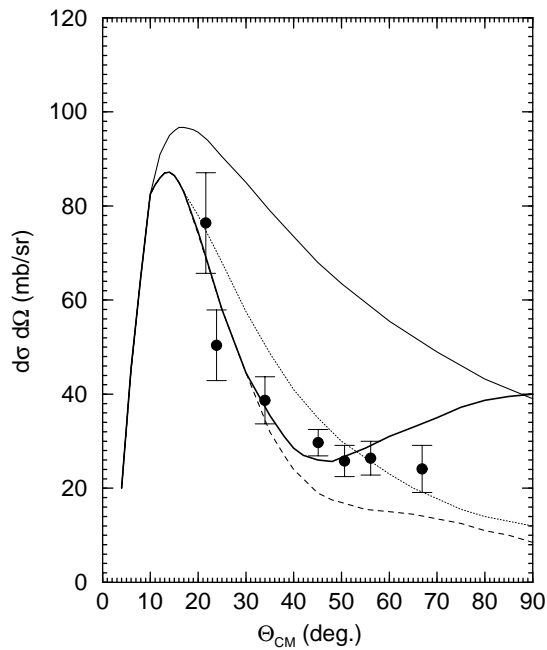


FIG. 2. Experimental angular distribution for ^8B breakup as measured in this paper, compared with the calculations presented in Ref. [13]. The various curves are discussed in the text.

have taken the average of the yield measured in the two telescopes.

It is obvious from inspection of the experimental angular distribution (see Fig. 3) that our data are completely inconsistent with the large amplitude peak in the vicinity of 70° – 90° which was a prominent feature of both first-order theories [10,11]. Very recently, however, two calculations [13,14] that incorporate higher-order effects have been published, and they display a much different large-angle behavior. Esbensen and Bertsch [13] performed a dynamical calculation that followed the time evolution of the valence proton wave function to all orders in the Coulomb and nuclear fields of the target. Their results are compared with our data in Fig. 2. The dotted curve corresponds to pure Coulomb breakup while the dashed curve, which includes nuclear effects, can be directly compared with the calculations presented in Refs. [10] and [11]. It can be seen that the higher-order couplings have completely eliminated the large-angle peak predicted by these first-order theories. Nevertheless, it is also clear that Coulomb-nuclear interference at very large distances, due to the extended nature of the “proton halo” in ^8B , still plays an important role in accounting for the experimental data.

Two other curves also appear in Fig. 2. The thin solid line illustrates pure Coulomb excitation under the usual “pointlike” assumption. The dotted curve, which is much closer to the experimental data, is the correct pure-Coulomb-excitation calculation which takes into account the extended size of the valence proton orbital of the projectile. This result emphasizes the importance of incorporating the unusual structure of ^8B in all aspects

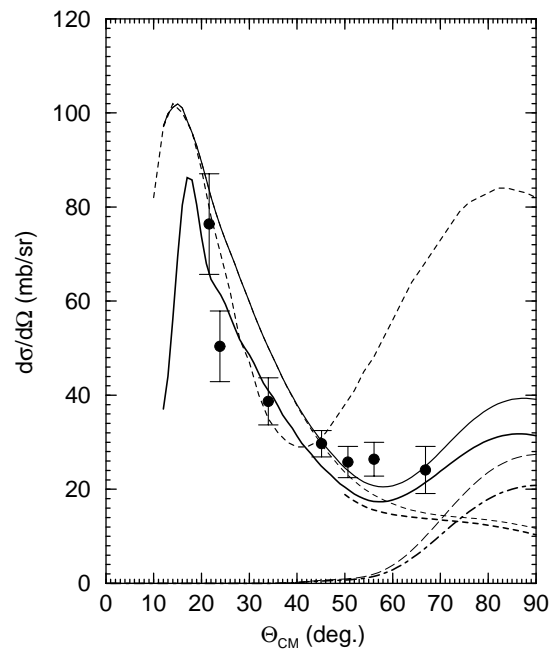


FIG. 3. The experimental data compared with the calculation of Nunes *et al.* (Refs. [14,15]). The various curves are discussed in the text, except for the two dotted-dashed curves. These are the separate contributions of transfer reactions as calculated in the structure model of Refs. [8,9]. The dashed curve with peaks at 15° and 85° is the first-order calculation [10].

of the reaction dynamics as first discussed in Ref. [10]. (Note that the pointlike approximation is still valid for neutron-halo nuclei since the relevant distance in this case is that between the core and the center of mass of the halo nucleus, which is still small.) The thick solid curve includes, in addition to breakup, the effect of nucleon transfer from the projectile to the target. This is the calculation that is most appropriate for comparison with our data since we do not distinguish transfer from breakup. The large-angle peak is partially restored (but transfer was not included in the calculations presented in Refs. [10] and [11] so the computed transfer yield should be added to the angular distributions presented there). The present data suggest that proton transfer may have been somewhat overestimated in Ref. [13]. Nevertheless, the overall agreement between theory and experiment is remarkable, especially considering that there has been no renormalization of the predicted absolute cross section.

Nunes and Thompson [14] have also included higher-order effects, using the coupled discretized continuum channels (CDCC) method combined with the structure model of Esbensen and Bertsch [8]. The advantage of this approach was that they were able to explicitly show that the vanishing of the large-angle peak results directly from the coupling among continuum states. Nunes [15] has added proton transfer to this calculation and the result appears as the thick solid line in Fig. 3. She has also repeated the calculation using the structure model of Kim *et al.* [9] which, as mentioned above, has both a larger

$E1$ and $E2$ component. The result is shown as the thin solid curve in Fig. 3. In general, the data favor the CDCC calculation using the wave function of Ref. [8], but the differences are small.

In conclusion, the angular distribution of the breakup of ${}^8\text{B}$ into ${}^7\text{Be} + p$ on a ${}^{58}\text{Ni}$ target was measured over a wide range of angles at a laboratory energy of 25.75 MeV. Time-of-flight information allowed us to unambiguously separate the ${}^7\text{Be}$ fragments coming from the breakup process, considerably improving on a previous measurement [2]. The data are completely inconsistent with first-order reaction theories [10,11] which predict a large amplitude nuclear dominated peak in the cross section at a center-of-mass angle of 70° – 90° . However, recent calculations [13–15] incorporating higher-order effects are in excellent agreement with experiment. In these calculations, the spurious peak is eliminated by continuum-continuum couplings. Coulomb-nuclear interference at very large distances, and the need to account for the extended size of the valence proton wave function in computing Coulomb breakup, are important features of both calculations. Thus, the present data may well be the best evidence yet of an exotic proton halo structure for ${}^8\text{B}$. This has been a matter of some controversy, since reaction cross section measurements at relativistic energies by Tanihata *et al.* [16] displayed little or no enhancement, while similar measurements at intermediate energies by Warner *et al.* [17] and Negoita *et al.* [18] showed a rather substantial enhancement. (Enhancements in the reaction cross sections were the first signature of the neutron halo.) The present data illustrate that finite-size effects and nuclear-Coulomb interference at very large distances, well outside the normal range of the nuclear force, are crucial features for the understanding of ${}^8\text{B}$ reactions at near-barrier and sub-barrier energies.

The original goal of the experiment described in Ref. [2] was to obtain a model-independent measurement of the $E2$ component in ${}^8\text{B}$ breakup and the astrophysical S factor S_{17} for proton capture on ${}^7\text{Be}$ at solar energies. In light of the discussion above, it appears that this will be very difficult. Even at the farthest forward angles measured in this experiment, corresponding to a distance of closest approach greater than 30 fm, Coulomb-nuclear (and multiple-Coulomb-excitation) interference effects are important. While our data are consistent with the results of Davids *et al.* [4], in the sense that the same structure model provides good predictions for both data sets, this conclusion is model dependent. On the other hand, the results from Ref. [4] are also model dependent and the applicability of first-order perturbation theory and the point-Coulomb approximation, used there and in the analysis of breakup data at intermediate energies [1,3], should be reinvestigated.

There does appear to be some sensitivity to the various structure models in our data. The wave function of Kim *et al.* [9], which has the larger S_{17} and $E2$ components, does not fit the data as well as other models, but the differences are too small to allow us to make any definitive statements about either quantity at this time.

Finally, the interactions of exotic, weakly bound nuclei at near- and sub-barrier energies will increasingly be investigated as the next generation of radioactive ion beam facilities using the ISOL (isotopic separator on-line) technique become available. It is comforting that there exist at least two successful theoretical approaches to the difficult problem of understanding low-energy reaction dynamics of weakly bound nuclei. We have shown that the information obtained from these reactions is complementary to that obtained from studies at intermediate and relativistic energies.

One of us (V.G.) was supported by the Fundação de Amparo a Pesquisa do Estado de São Paulo, Brazil, while on leave from the Universidade Paulista (UNIP). This work was supported by the National Science Foundation under Grants No. PHY94-01761, No. PHY95-12199, No. PHY97-22604, No. PHY98-04869, and No. PHY99-01133.

-
- [1] T. Motobayashi *et al.*, Phys. Rev. Lett. **73**, 2680 (1994).
 - [2] J. von Schwarzenberg, J.J. Kolata, D. Peterson, P. Santi, M. Belbot, and J.D. Hinnefeld, Phys. Rev. C **53**, R2598 (1996).
 - [3] T. Kikuchi *et al.*, Phys. Lett. B **391**, 261 (1997).
 - [4] B. Davids *et al.*, Phys. Rev. Lett. **81**, 2209 (1998).
 - [5] N. Iwasa *et al.*, Phys. Rev. Lett. **83**, 2910 (1999).
 - [6] K. Langanke and T.D. Shoppa, Phys. Rev. C **49**, R1771 (1994).
 - [7] M. Gai and C. A. Bertulani, Phys. Rev. C **52**, 1706 (1995).
 - [8] H. Esbensen and G.F. Bertsch, Phys. Lett. B **359**, 13 (1995); Nucl. Phys. **A600**, 37 (1996).
 - [9] K.H. Kim, M.H. Park, and B.T. Kim, Phys. Rev. C **35**, 363 (1987).
 - [10] F.M. Nunes and I.J. Thompson, Phys. Rev. C **57**, R2818 (1998).
 - [11] C.H. Dasso, S.M. Lenzi, and A. Vitturi, Nucl. Phys. **A639**, 635 (1998).
 - [12] M.Y. Lee *et al.*, Nucl. Instrum. Methods Phys. Res., Sect. A **422**, 536 (1999).
 - [13] H. Esbensen and G.F. Bertsch, Phys. Rev. C **59**, 3240 (1999).
 - [14] F.M. Nunes and I.J. Thompson, Phys. Rev. C **59**, 2652 (1999).
 - [15] F.M. Nunes (private communication).
 - [16] I. Tanihata *et al.*, Phys. Lett. B **206**, 592 (1988).
 - [17] R.E. Warner *et al.*, Phys. Rev. C **52**, R1166 (1995).
 - [18] F. Negoita *et al.*, Phys. Rev. C **54**, 1787 (1996).